Design and Analysis of Receiver Filters for Multiple Chip-Rate DS-CDMA Systems

Radha Srinivasan, Urbashi Mitra, *Member, IEEE*, and Randolph L. Moses, *Senior Member, IEEE*

***Abstract*— As multimedia applications proliferate, there is a desire to provide wireless transport to information streams with inherently different data rates. Direct-sequence code division multiple access (DS-CDMA) is a natural multiple-access strategy for multiple data-rate systems. Recent work on multirate DS-CDMA receivers has focused on signal-processing techniques, which detect all users of all rates simultaneously. In the current work, multirate users have multiple bandwidths. Thus, it is proposed to exploit bandwidth differences to achieve frequency-based rate separation followed by single-rate detection schemes. Such a methodology enables a tradeoff between receiver complexity and performance. The performance of the proposed filters and receivers are derived for both a modified matched filter and modified decorrelator employing rate separation. Performance of a multirate CDMA overlay system is evaluated. In addition, chip pulse shaping for wide-band users is developed to improve performance for narrow-band users for the overlay system.**

***Index Terms*—Direct signal code division multiple access (DS-CDMA), multimedia services, multirate systems, multiuser detection, overlay systems, pulse shaping, variable chipping rate CDMA, Wiener filters.**

I. Introduction

DIRECT-SEQUENCE code division multiple access (DS-CDMA) is a promising technique for providing multiuser access in wireless systems. Relative to other multiple-access schemes, CDMA can increase the number of potential users in bursty or fading channels making it attractive for applications such as mobile cellular telephony and personal communication systems (PCS).

In the last few years, multiuser receiver developments for CDMA-based communications (see, e.g., [1]–[5]) have primarily focused on single-rate systems where all users transmit information at the same data rate. With the exploding growth of cellular communication systems, there has been much interest in advanced PCS. PCS promises to offer wireless transport for a variety of data sources such as images (facsimiles), video, data, as well as voice. Different information sources will have inherently different data rates and bandwidths. Therefore, in order to have a wireless system that will serve these diverse sources, it is desirable to develop multiple data-rate systems.

We propose to explore the feasibility of rate-separation via frequency-based techniques. In this work, we shall develop multirate multiuser receivers that first perform user separation by rate, followed by single-rate multiuser detection, and analyze their performance. Multirate CDMA systems have been investigated from different perspectives. The appropriate choice of the chip rate, chip pulse shape, processing gain, number of codes, and modulation format is considered in [6]–[10]. Access methodologies and their comparison are presented in [13] and [14]. Much of the prior work on receiver design also assumed a constant chipping rate. In the current work, we will assume a fixed processing gain for each user but varying chipping rates (also seen in [14] and [28]). In [28], new methods for updating adaptive minimum-mean squared-error receivers for a multirate overlay system was considered. Overlay systems will also be considered herein to improve performance.

Proposed third-generation DS-CDMA standards consider a variety of methods for accomplishing multiple data rates. Variable spreading length (constant chip rate), multicode, and discontinuous transmission schemes are discussed in [12] and [11] in reference to UMTS/IMT2000 and W-CDMA. In [11], multiple chip rates are also specified for the radio link. It is anticipated that future standards will incorporate hybridized versions of the different multirate access schemes to tailor the data rate to the application. While there has been initial emphasis on variable spreading length and multicode methods for multirate DS-CDMA, there are pragmatic reasons to investigate multiple chip-rate methods. Having multiple chip rates enables low-rate users to have only limited hardware needs. Thus, a low-rate voice user does not need to have the capability of transmitting at the same chipping rate as a video user.

Among the receivers proposed for multirate CDMA systems are the conventional receiver [6], decorrelator-based receivers [15], [16], the optimum receiver [17], multistage receivers, and receivers based on successive interference cancellation [18]. Most of the previously proposed receivers were designed to directly operate on the complete received signal, which consists of the multirate signals without any preprocessing. This causes the receiver structure to be complex, with the complexity increasing with the total number of virtual users in the system. Also in some cases, the receiver requires knowledge of the particular choice of spreading codes of each of the active users. This motivates us to consider separation of users of different rates and process them with single-rate detectors that have low complexity.

The contribution of this paper is to propose a class of receivers that preprocess the received multirate signal into several single-rate signals. In this way, a multirate problem is decomposed into multiple single-rate problems. Due to the

Manuscript received October 1, 1998; revised April 15, 1998.

R. Srinivasan is with Nokia Research Centre, Irving, TX 75039 USA.

U. Mitra and R. L. Moses are with the Department of Electrical Engineering, The Ohio State University, Columbus, OH 43210 USA.

Publisher Item Identifier S 0733-8716(99)09090-3.

assumption of different chipping rates for users of different data rates, the users will have different bandwidths. These bandwidth differences can be exploited for frequency-based rate separation. The notion of frequency-based narrow-band interference suppression of [20] will be extended to multirate CDMA systems. Three rate-separating preprocessors will be considered: Wiener filters, high- and low-pass filters, and some new filters (which we will call *Q-filters*) based on minimizing interference. Once rate separation has been accomplished, previously proposed multiuser receivers for single-rate communications can be applied (the matched filter and the decorrelating detector [1] are considered here). Note that we will incur a loss in performances as we do not model all the users; this work is, in part, a feasibility study to assess performance loss versus reduction in receiver complexity. The probability of error for these different schemes will be calculated for an asynchronous dual-rate scenario. The proposed receiver structure is suited to be used both at the mobile and at the base station. Also, for this receiver, the rate ratio is not required to be an integer, unlike most of the previously proposed receiver designs [15] where this property is necessary. While the focus of the paper is on dual-rate systems, the receiver can be extended for multirate systems. As an example, we have also considered a system with three different rates; performance curves for a selected set of scenarios are presented.

For efficient utilization of the allotted bandwidth and to improve the performance of the low-rate users, a multirate CDMA overlay situation, where different sets of low-rate users modulated onto different carriers are overlaid on the high-rate users, will be considered. The performance of the proposed receiver for such a system will be studied. We will see that in such an overlay system where the high-rate users have a raised cosine spectra, certain sets of low-rate users suffer in performance due to the strong high-rate interference, while the other sets experience less high-rate interference. Therefore, to have all sets of low-rate users experience equal amounts of out-of-rate interference, design of the chip pulse shape of high-rate users will be investigated.

This paper is organized as follows. Section II describes the received signal and the dual-rate communication scenario. Section III proposes the receiver structure, which uses a frequency-based rate-separation technique and gives the design of a few rate-separating filters. Probabilities of error for low- and high-rate users are derived, and numerical results for a dual-rate asynchronous system are presented. Section IV investigates the performance of the proposed receiver in a CDMA overlay system. It also includes the design of high-rate chip pulse shapes and analyzes the improvement in performance. In Section V, numerical results are provided. Section VI summarizes and concludes this paper.

II. PRELIMINARIES

We shall consider an asynchronous dual-rate DS-CDMA system with K_0 low-rate users and K_1 high-rate users. We present a dual-rate system to maintain notational simplicity, although the receiver systems proposed herein, and all derivations, can easily be extended to multirate systems (numerical results for a three-rate system are provided in Section V). In this work, we shall also assume coherent reception. Although the rate-separation filters proposed in this paper are applicable to multipath channels, we will assume nonmultipath channels in our analysis. The system model considered here is for the uplink where signals from several mobiles arrive at the base station. In Section III, we propose receiver structures that can be used at the base station to detect the signals from different users. To implement the receivers, knowledge of the spreading waveforms of all users and their delays is required. The spectra of the users required to design the rate-separation filter can be obtained from the spreading waveforms. It should be noted that some of the proposed receivers can also be used at the mobile, with knowledge of the frequency bands or the spectra of all users. In order to implement the Wiener filter, the amplitudes of all users should also be known. To ease this requirement, a Wiener filter designed on the assumption of unity-received power for each rate is also considered.

To preview the assumptions made in our study, we shall consider systems with the following characteristics:

1) dual-rate systems (for clarity);
2) multiple chip rates;
3) binary phase shift keying (BPSK) modulation;
4) Gold sequences;
5) additive white Gaussian noise channels with no multipath.

We next explicitly describe the system model and the impact of the assumptions above on this model. The subscript g will refer to low-rate users $(g = 0)$ or high-rate users $(g = 1)$. The bit duration of a user of type g is denoted by T_g. The rate ratio M is defined as T_0/T_1 to be an integer, for ease of calculation. The reception schemes are not at all dependent on M being an integer; however, it greatly simplifies notation to presume that M is an integer, and so we adopt this convention herein. The received baseband signal over $2B+1$ bits of the low-rate users can be expressed as

$$\begin{aligned} r(t) = &\sum_{k=1}^{K_0} \sum_{i=-B}^{B} a_{k,0} b_{k,0}[i] s_{k,0}(t - iT_0 - \tau_{k,0}) \\ &+ \sum_{k=1}^{K_1} \sum_{i=-B}^{B} \sum_{m=0}^{M-1} a_{k,1} b_{k,1}^{m}[i] \\ &s_{k,1} \cdot (t - (iM + m)T_1 - \tau_{k,1}) + n(t) \end{aligned} \quad (1)$$

where $a_{k,0}$ and $b_{k,0}[i]$ denote the received amplitude and received bit, respectively, during the ith bit interval for the kth low-rate user. Similarly, $a_{k,1}$ and $b_{k,1}^{m}[i]$ denote the kth high-rate user's received amplitude and received bit during the mth subinterval of the ith low-rate bit interval. Assuming BPSK, the transmitted data bits $b_{k,g}^{m}[i]$ are independent and identically distributed (i.i.d.), taking on values from $\{-1, +1\}$ with equal probability. The signature waveforms are denoted by $s_{k,0}(t)$ and $s_{k,1}(t)$ for the kth low- and high-rate users, respectively. The delay of the kth user of group g, with respect to the base station's symbol timing, is denoted by $\tau_{k,g}$. For simplicity, we will assume that the delays are within the high-rate bit interval, i.e., $\tau_{k,g} \in [0, T_1)$. It is assumed that the delays of all active users are known to the receiver. In this dual-rate system, we use a constant processing gain N for all users and let the chip rate vary according to the bit rate [14]. If T_{c_g} is the chip duration of the gth rate user, then $T_{c_0}/T_{c_1} = M$. The signature waveforms can be expressed as

$$s_{k,g}(t) = \sum_{n=1}^{N} \frac{1}{\sqrt{N}} c_{k,g}(n) p_g(t-(n-1)T_{c_g}), \quad t \in [-\tilde{T}_g, T_g + \tilde{T}_g] \tag{2}$$

where $c_{k,g}(n) \in \{-1, 1\}$ denotes the signature sequence of user k of group g and $p_g(t)$ is the chip pulse shape of length $T_{c_g} + 2\tilde{T}_g$. The extreme chips cause intersymbol interference (ISI) of duration $\tilde{T}_g$. It should be noted that the interchip interference introduced by all chips other than the extremes are absorbed into the signature waveform. We shall assume essentially band-limited chip shapes. In particular, $p_g(t)$ is assumed to have a raised cosine spectral pulse [19] and is defined by

$$p_g(t) = \begin{cases} \text{sinc}((2t - T_{c_g})/T_{c_g}) \dfrac{\cos(\pi\alpha(2t - T_{c_g})/T_{c_g})}{1 - 4\alpha^2(2t - T_{c_g})^2/T_{c_g}^2}, \\ \quad -\tilde{T}_g \le t \le T_{c_g} + \tilde{T}_g \\ 0, \quad \text{elsewhere} \end{cases} \tag{3}$$

where α is the *rolloff* factor, which takes values in the range $0 \le \alpha \le 1$. These pulses are essentially band-limited as opposed to rectangular pulses, which have much higher spectral leakage. The excess bandwidth can be calculated as $\alpha \cdot 100\%$. For our study, we use $\alpha = 0.3$, which corresponds to an excess bandwidth of 30%, and we set $\tilde{T}_g = 2.5T_{c_g}$. The energy of the pulse $p_g(t)$ is normalized so that

$$\int_{-\tilde{T}_g}^{T_g + \tilde{T}_g} (s_{k,g}(t))^2 \, dt = 1, \quad g = 0, 1; \quad k = 1, \ldots, K_g. \tag{4}$$

Finally, the additive white Gaussian noise in (1) is denoted by $n(t)$, with zero mean and autocorrelation function $R(t, s) = \sigma^2 \delta(t - s)$.

III. Receiver Structures

In this dual chip-rate system, users with different rates have different bandwidths, and therefore we can exploit this difference to separate users of different rates. Simple filters such as low-pass, high-pass and Wiener filters can achieve frequency-based rate separation. Thus, the dual-rate problem is decomposed into two single rate problems to which we can apply existing detection schemes with appropriate modifications. The proposed receiver system can be described by the block diagram in Fig. 1(a). We observe that the receiver structure can easily be extended for a multirate system. We begin by describing the filter choices and then review the single-rate multiuser receivers, modified to include other-rate interference and filter effects. Due to the linearity of the receiver, it is straightforward to calculate the probability of error. In the sequel, new filter structures are explored.

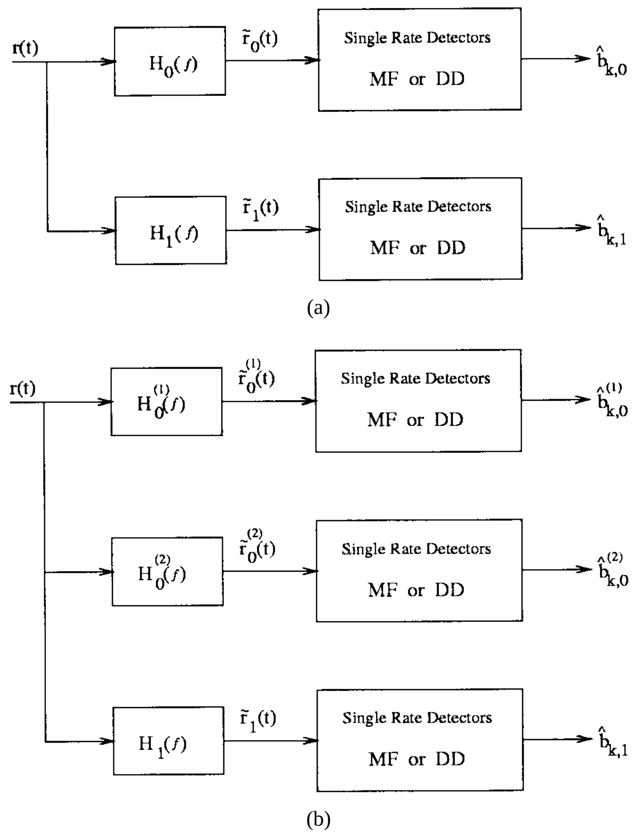

Fig. 1. (a) Receiver bit structure for dual-rate DS-CDMA system. (b) Receiver for dual rate DS-CDMA system in an overlay situation with two sets of low-rate users.

A. Filter Choices

Narrow-band interference suppression for direct-sequence spread-spectrum overlay systems is a well-explored problem in the literature [20]–[23]. Much of the prior work [20]–[22] used Wiener-type filters employing tap delay line structures to first predict and then subtract out the narrow-band interference. Here, we will consider some interference suppression filters for a multirate DS-CDMA system, borrowing from the narrow-band interference suppression literature. Simple high- and low-pass filters as well as Wiener filters are considered. The performance of these filters is numerically evaluated in Section V.

1) High- and Low-Pass Filters: The difference in the bandwidth between users of different rates suggests the use of simple filters, such as high-pass and low-pass filters, for separating the high-rate and low-rate users. The cutoff frequencies of the filters are related to the rolloff factor α and the low-rate chip duration T_{c_0} as $f_{\text{cut-off}} = (1 + \alpha)/T_{c_0}$.

The filtering operation introduces intersymbol interference (ISI), which poses a constraint on the length of the filter. To limit the ISI to only adjacent bits, the filter length should be less than the bit duration of the high-rate user.

2) Wiener Filter: It has been shown in [24] that suppression of multiple access interference in a single-rate DS-CDMA system using Wiener filters gives better performance than a single stage of parallel cancellation. In this dual-rate system, to detect users of one rate, Wiener filters can be used to suppress the multiple access interference due to the users of the other rate. If g is the desired group of users, then the Wiener equation to suppress other rate users can be written as

$$H_g(f) = \frac{a_g S_g(f)}{a_0 S_0(f) + a_1 M S_1(f) + S_N(f)}, \qquad g = 0, 1 \tag{5}$$

where $a_g = \Sigma_{k=1}^{K_g} a_{k,g}^2$, is the effective amplitude squared of all users in rate g ($g = 0, 1$) and $S_N(f) = \sigma^2$, $\forall f$. Due to the assumption of independent data bits and independent chips with unit variance, the power spectral density (PSD) of each user of rate g is given by the magnitude squared of the Fourier transform of the pulse shape $p_g(t)$, i.e., $S_g(f) = |\mathcal{F}\{p_g(t)\}|^2$, where $\mathcal{F}$ denotes the Fourier transform operator. The raised cosine frequency characteristics for a pulse of infinite length is given as

$$S_{rc}(f) = \begin{cases} \dfrac{T_{c_g}}{2}, & 0 \le |f| \le \dfrac{1-\alpha}{T_{c_g}} \\ \dfrac{T_{c_g}}{4}\left[1 + \cos\dfrac{\pi T_{c_g}}{2\alpha}\left(|f| - \dfrac{1-\alpha}{T_{c_g}}\right)\right], & \dfrac{1-\alpha}{T_{c_g}} \le |f| \le \dfrac{1+\alpha}{T_{c_g}} \\ 0, & |f| > \dfrac{1+\alpha}{T_{c_g}}. \end{cases} \tag{6}$$

Let the power spectral density be written in terms of the Fourier transform of the infinite pulse as $S_{\rm rc}(f) = X_{\rm rc}(f)X_{\rm rc}^*(f)$. Since $p_g(t)$ has finite duration $T_{c_g} + 2T_g$ and is set to zero outside this interval, the Fourier transform of $p_g(t)$ can be obtained by convolving $X_{\rm rc}(f)$ with the Fourier transform $W(f)$ of a rectangular window. Thus, $S_g(f) = |X_{\rm rc}(f) * W(f)|^2$. Note that in this paper, the notation $(\cdot)^*$, $(\cdot)^T$ and $(\cdot)^{-1}$ is used to represent conjugate, transpose, and inverse operations, respectively.

If one wishes to have a Wiener filter that is independent of the amplitude of the users, the corresponding Wiener equation is given by

$$H_g(f) = \frac{S_g(f)}{\alpha_0 S_0(f) + \alpha_1 S_1(f) + \alpha_N S_N(f)} \tag{7}$$

where α_0, α_1, and α_N are constants that can be chosen arbitrarily and still yield a fixed Wiener filter. We have chosen $\alpha_0 = \alpha_1 = \alpha_N = 1$. This fixed filter has an advantage over the Wiener filter in (5) as we do not have to estimate the amplitudes of the users. Note that this formulation of the filter represents a mismatch between the actual system parameters and how the system is modeled to derive the filter. We will see, however, that robust performance is still offered by this filter design. We refer to this modified filter design as the amplitude independent Wiener filter. Technically, this filter is not a Wiener filter.

The Wiener equation in (5) can be modified for a multirate system with G different rates as

$$H_g(f) = \frac{a_g M_g S_g(f)}{\sum_{l=0}^{G-1} a_l M_l S_l(f) + S_N(f)} \tag{8}$$

where $M_l = T_l/T_0$.

B. Performance Analysis

We first describe the filtered signal and then consider two single-rate receivers. Let $\tilde{s}_{k,g}(t)$ denote the signature waveforms in (2) filtered by the rate-separation filter $H_g(f)$. The filtered waveform can be written as

$$\tilde{s}_{k,g}(t) = \begin{cases} \tilde{s}_{k,g}^r(t), & -T_1 \le t \le 0 \\ \tilde{s}_{k,g}^c(t), & 0 \le t \le T_1 \\ \tilde{s}_{k,g}^l(t), & T_1 \le t \le 2T_1 \\ 0, & \text{otherwise} \end{cases} \tag{9}$$

where the ISI due to the bits on the left and right are denoted by $\tilde{s}_{k,g}^l(t)$ and $\tilde{s}_{k,g}^r(t)$, respectively. Here, we assume that the length of the filter is less than one high-rate bit interval T_1. The center portion of the filtered signal is denoted by $\tilde{s}_{k,g}^c(t)$ and is essentially the modified spreading waveform of the user, which will be used in the single-rate detector. The signal at the output of the filter for the gth rate over the ith low-rate bit interval (i.e., $iT_0 \le t \le (i+1)T_0$) can be written as

$$\begin{aligned} \tilde{r}_g(t) = {} & \sum_{k=1}^{K_0} a_{k,0} \Bigg\{ \sum_{m=-1}^{1} \tilde{s}_{k,0}(t - iT_0 - mT_0 - \tau_{k,0}) \\ & \cdot b_{k,0}[i+m] \Bigg\} \\ & + \sum_{k=1}^{K_1} a_{k,1} \Bigg\{ \sum_{m=M-2}^{M-1} \tilde{s}_{k,1}(t - (i-1)T_0 \\ & - mT_1 - \tau_{k,1}) b_{k,1}^m[i-1] \\ & + \sum_{m=0}^{M-1} \tilde{s}_{k,1}(t - iT_0 - mT_1 - \tau_{k,1}) \\ & \cdot b_{k,1}^m[i] + \tilde{s}_{k,1}(t - (i+1)T_0 - \tau_{k,1}) \\ & \cdot b_{k,1}^0[i+1] \Bigg\} + \tilde{n}(t) \end{aligned} \tag{10}$$

where $\tilde{n}(t)$ is the colored Gaussian noise at the output of $H_g(f)$ and has power spectral density $\sigma^2|H_g(f)|^2$. Considering the low-rate users, the multiple access interference will be caused by bits $b_{k,0}[i-1]$ and $b_{k,0}[i]$ for positive values of the delays $\tau_{k,0}$. The ISI from the right is caused by $b_{k,0}[i+1]$. It should be noted that there will be no ISI due to $b_{k,0}[i-2]$, as we have assumed that the filter length and the delays are less than T_1. For the high-rate users, the MAI will be caused by bits $b_{k,1}^{M-1}[i-1]$ and $b_{k,1}^m[i]$, $m = 0, \ldots, M-1$. The ISI from the left and the right is caused by bits $b_{k,1}^{M-2}[i-1]$ and $b_{k,1}^0[i+1]$, respectively. Here again we have assumed positive delays $\tau_{k,1}$.

1) Matched Filter: We first consider the conventional matched filter. This receiver is simply a filter that correlates the filtered signal with the modified spreading waveform of the user of interest. While it is clear that the matched filter is a suboptimal multiuser receiver [1], determination of its performance enables the evaluation of the preprocessing filter's ability to suppress out-of-rate interference. Without loss of generality, let us assume that $\tau_{k,0} = 0$. Then, the sampled output of the matched filter for the ith bit of the kth low-rate user at the symbol rate, $i = -B, \ldots, B$, is

$$y_{k,0}[i] = \int_{iT_0}^{(i+1)T_0} \tilde{r}_0(t)\tilde{s}^c_{k,0}(t - iT_0)\,dt \tag{11}$$

$$\begin{aligned} &= \sum_{j=1}^{K_0}\sum_{m=-1}^{1} a_{j,0}\tilde{\rho}^m_{k,0;j,0} b_{j,0}[i+m] \\ &\quad + \sum_{j=1}^{K_1} a_{j,1}\Bigg\{\sum_{m=-2}^{-1}\tilde{\rho}^m_{k,0;j,1} b^{M+m}_{j,1}[i-1] \\ &\quad\quad + \sum_{m=0}^{M-1}\tilde{\rho}^m_{k,0;j,1} b^m_{j,1}[i] \\ &\quad\quad + \tilde{\rho}^M_{k,0;j,1} b^0_{j,1}[i+1]\Bigg\} + \tilde{n}_{k,0}[i] \end{aligned} \tag{12}$$

where $\tilde{r}_g(t)$ is the filtered signal at the output of the filter for group g and $\tilde{n}_{k,0}[i]$ is the zero mean colored Gaussian noise at the output of the matched filter. If we use $\Omega = 2\pi f$ instead of f, we can write the variance of the noise $\tilde{n}_{k,0}[i]$ as

$$\tilde{\sigma}^2_{k,g} = \frac{\sigma^2}{2\pi}\int_{-\infty}^{\infty} |H_g(\Omega)\tilde{S}^c_{k,g}(\Omega)|^2\,d\Omega \tag{13}$$

where $\tilde{S}^c_{k,g}(\Omega)$ is the Fourier transform of $\tilde{s}^c_{k,g}(t)$. The cross-correlation functions $\tilde{\rho}^m_{k,0;j,0}$ and $\tilde{\rho}^m_{k,0;j,1}$ are defined as follows

$$\tilde{\rho}^m_{k,0;j,0} = \int_0^{T_0} \tilde{s}^c_{k,0}(t)\tilde{s}_{j,0}(t - mT_0 - \tau_{j,0})\,dt \tag{14}$$

$$\tilde{\rho}^m_{k,0;j,1} = \int_0^{T_0} \tilde{s}^c_{k,0}(t)\tilde{s}_{j,1}(t - mT_1 - \tau_{j,1})\,dt. \tag{15}$$

Though the cross-correlations depend on the delays, we will not include the delays in the notation for ease of readability.

Similarly, the sampled output of the matched filter for the $(p = iM + x)$th bit of the kth high-rate user $(i = -B, \ldots, B;\ x = 0, \ldots, M-1)$ assuming $\tau_{k,1} = 0$ is given by

$$y_{k,1}[p] = \int_{pT_1}^{(p+1)T_1} \tilde{r}_1(t)\tilde{s}^c_{k,1}(t - pT_1)\,dt \tag{16}$$

$$\begin{aligned} &= \sum_{j=1}^{K_1}\sum_{m=-2}^{1} a_{j,1}\tilde{\rho}^m_{k,1;j,1} b_{j,1}[p+m] \\ &\quad + \sum_{j=1}^{K_0}\sum_{m=-1}^{1} a_{j,0}\tilde{\rho}^{m,x}_{k,1;j,0} b_{j,0}[i+m] \\ &\quad + \tilde{n}_{k,1}[i] \end{aligned} \tag{17}$$

where $\tilde{\rho}^{-2}_{k,1;k,1} = 0$. Note that $\tilde{\rho}^{-1,x}_{k,1;j,0} = 0$ for $x = 2, \ldots, M-1$. Here, the cross-correlations are defined as

$$\tilde{\rho}^{m,x}_{k,1;j,0} = \int_0^{T_1} \tilde{s}^c_{k,1}(t)\tilde{s}_{j,0}(t - mT_0 + xT_1 - \tau_{j,0})\,dt \tag{18}$$

$$\tilde{\rho}^m_{k,1;j,1} = \int_0^{T_1} \tilde{s}^c_{k,1}(t)\tilde{s}_{j,1}(t - mT_1 - \tau_{j,1})\,dt. \tag{19}$$

The bit decision for the ith bit of the kth low-rate user is $\hat{b}_{k,0}[i] = \text{sgn}(y_{k,0}[i])$. The probability of error for the kth low-rate user can be written as[1]

$$P^{\text{MF}}_{k,0} = \frac{1}{2^{3K_0+(M+3)K_1-1}}\sum_{b_{k,0}[i]=1} Q\left(\frac{y_{k,0}(\underline{b})}{\tilde{\sigma}_{k,0}}\right) \tag{20}$$

where $y_{k,0}(\underline{b})$ is as defined in (12) without the noise term; and the elements of $\underline{b}$ refer to all the b elements in (12). The summation is over all possible combinations of the transmitted bits $b_{j,g}$; however j with the desired user's bit $b_{k,0}[i]$ as 1. Similarly, the bit decision for the pth bit of the kth high rate user is $\hat{b}_{k,1}[p] = \text{sgn}(y_{k,1}[p])$. The probability of error for the kth high-rate user is

$$P^{\text{MF}}_{k,1} = \frac{1}{M}\sum_{x=0}^{M-1}\frac{1}{2^{3K_0+4K_1-1}}\sum_{b_{k,1}[p]=1} Q\left(\frac{y_{k,1}(\underline{b})}{\tilde{\sigma}_{k,1}}\right) \tag{21}$$

where $y_{k,1}(\underline{b})$ is similarly defined from (17).

2) Decorrelating Detector: To consider a more sophisticated multiuser receiver, we look to the decorrelating detector [1]. We shall focus on the one-shot decorrelating detector [27]. Without loss of generality, let us assume that user 1 of group g is the desired user. Effectively, we have a $(2K_g - 1)$-user "synchronous" channel with ISI and multiple access interference from users of the other group. The gth rate interferers have signature waveforms

$$\bar{s}^L_{k,g}(t) = \begin{cases} \tilde{s}_{k,g}(t + T_g - \tau_{k,g}), & 0 \le t \le T_g \\ 0, & \text{else} \end{cases} \tag{22}$$

$$\bar{s}^R_{k,g}(t) = \begin{cases} \tilde{s}_{k,g}(t - \tau_{k,g}), & 0 \le t \le T_g \\ 0, & \text{else} \end{cases} \tag{23}$$

for $k = 2, \ldots, K_g$.

A bank of $2K_g - 1$ filters matched to the above signature waveforms is formed. The output of the matched filters for all low-rate users can be written in matrix form as

$$\begin{aligned} \underline{\check{y}}_{MF(0)}[i] &= \check{R}_{00}\check{A}_0\underline{\check{b}}_0 + \check{R}_{00}[1]A_0\underline{b}_0[i+1] \\ &\quad + \sum_{m=-2}^{-1}\check{R}_{01}[m]A_1\underline{b}_1^{M+m}[i-1] \\ &\quad + \sum_{m=0}^{M-1}\check{R}_{01}[m]A_1\underline{b}_1^m[i] \\ &\quad + \check{R}_{01}[M]A_1\underline{b}_1^0[i+1] + \underline{\check{n}}_0 \end{aligned} \tag{24}$$

where $\check{A}_g$ is a diagonal matrix whose diagonal elements are the amplitudes of the effective $2K_g - 1$ users at rate g (i.e., $\check{A}_g = \text{Diag}[a_{1,g}\ a_{2,g}\ a_{2,g}\ a_{3,g} \ldots a_{K_g,g}\ a_{K_g,g}]$) and A_g is as defined before. The cross-correlation matrices are defined as

$$[\check{R}_{\text{gg}}]_{i,j} = \int_0^{T_g}\check{s}_{i,g}(t)\check{s}_{j,g}(t)\,dt, \qquad g = 0, 1 \tag{25}$$

$$[\check{R}_{g1}[m]]_{i,j} = \int_0^{T_g}\check{s}_{i,g}(t)\tilde{s}_{j,1}(t - mT_1 - \tau_{j,1})\,dt, \quad g = 0, 1 \tag{26}$$

$$[\check{R}_{00}[1]]_{i,j} = \int_0^{T_0}\check{s}_{i,0}(t)\tilde{s}_{j,0}(t - T_0 - \tau_{j,0})\,dt \tag{27}$$

[1] $Q(x) = \int_x^\infty (1/\sqrt{2\pi})\exp\{-(v^2/2)\}\,dv$.

where

$$\breve{s}_{l,g}(t) = \begin{cases} \tilde{s}^c_{l,g}(t), & l = 1 \\ \overline{s}^L_{(l/2)+1,g}(t), & l \text{ even, } l \in [2, 2(K_g - 1)] \\ \overline{s}^R_{(l+1/2),g}(t), & l \text{ odd, } l \in [3, 2K_g - 1]. \end{cases} \quad (28)$$

The Gaussian noise vector $\underline{\breve{n}}_g$ has zero mean and covariance matrix $\breve{\Sigma}_g$ with

$$[\breve{\Sigma}_g]_{i,j} = (\sigma^2/2\pi) \int_{-\infty}^{\infty} (H_g(\Omega)\breve{S}_{i,g}(\Omega))(H_g(\Omega)\breve{S}_{j,g}(\Omega))^* \, d\Omega.$$

The vector $\underline{\breve{b}}_g$ is formed as

$$\underline{\breve{b}}_g = [b_{1,g}[i] \quad b_{2,g}[i-1] \quad b_{2,g}[i] \quad b_{3,g}[i-1] \quad \cdots \quad b_{K_g,g}[i-1] \quad b_{K_g,g}[i]]^T. \quad (29)$$

Similarly, the output of the matched filters for the pth bit of the high-rate users is given by

$$\underline{\breve{y}}_{\text{MF}(1)}[p] = \breve{R}_{11}\breve{A}_1\underline{\breve{b}}_1 + \sum_{m=-2,1} \breve{R}_{11}[m]A_1\underline{b}_1[p+m] + \sum_{m=-1}^{1} \breve{R}_{10}[m,x]A_0\underline{b}_0[i+m] + \underline{\breve{n}}_1 \quad (30)$$

where

$$[\breve{R}_{10}[m,x]]_{i,j} = \int_0^{T_1} \breve{s}_{i,1}(t)\tilde{s}_{j,0}(t - mT_0 - xT_1 - \tau_{j,0})\, dt \quad (31)$$

and all other matrices are defined as before.

In this work, we will consider a single-rate decorrelator that zero-forces all users of the desired group g other than the desired user, but not out-of-rate users. As a result of this, the residual MAI from out-of-rate users present after filtering could be enhanced. Using (24) and (30), the output of the decorrelating detector is

$$\underline{\breve{y}}_{\text{DD(g)}} = \breve{R}_{\text{gg}}^{-1}\underline{\breve{y}}_{MF(g)}. \quad (32)$$

The output of the decorrelator for the low-rate and high-rate users can be expanded as

$$\underline{\breve{y}}_{\text{DD}(0)}[i] = \breve{A}_0\underline{\breve{b}}_0 + \breve{R}_{00}^{-1} \cdot \Bigg(\breve{R}_{00}[1]A_0\underline{b}_0[i+1] + \sum_{m=-2}^{-1} \breve{R}_{01}[m]A_1\underline{b}_1^{M+m}[i-1] + \sum_{m=0}^{M-1} \breve{R}_{01}[m]A_1\underline{b}_1^{m}[i] + \breve{R}_{01}[M]\,A_1\underline{b}_1^0[i+1] + \underline{\breve{n}}_0\Bigg) \quad (33)$$

$$\underline{\breve{y}}_{\text{DD}(1)}[p] = \breve{A}_1\underline{\breve{b}}_1 + \breve{R}_{11}^{-1} \cdot \Bigg(\sum_{m=-2,1} \breve{R}_{11}[m]A_1\underline{b}_1[p+m] + \sum_{m=-1}^{1} \breve{R}_{10}[m,x]A_0\underline{b}_0[i+m]\Bigg) + \breve{R}_{11}^{-1}\underline{\breve{n}}_1. \quad (34)$$

The bit decisions for the kth user of group g is given by $\hat{b}_{k,g}[i] = \text{sgn}((\underline{y}_{\text{DD(g)}}[i])_k)$. Thus, the probabilities of the first low-rate and high-rate users are given as

$$P_{1,0}^{\text{DD}} = \frac{1}{2^{K_0+(M+3)K_1}} \sum_{\underline{b},(\underline{b})_1=1} Q\left(\frac{(\underline{\breve{y}}_{\text{DD}(0)}(\underline{b}))_1}{\sqrt{(\breve{R}_{00}^{-1}\breve{\Sigma}_0\breve{R}_{00}^{-1})_{1,1}}}\right) \quad (35)$$

$$P_{1,1}^{\text{DD}} = \frac{1}{M}\sum_{x=0}^{M-1} \frac{1}{2^{3K_0+2K_1}} \cdot \sum_{\underline{b},(\underline{b})_1=1} Q\left(\frac{(\underline{\breve{y}}_{\text{DD}(1)}(\underline{b}))_1}{\sqrt{(\breve{R}_{11}^{-1}\breve{\Sigma}_1\breve{R}_{11}^{-1})_{1,1}}}\right) \quad (36)$$

where $\underline{\breve{y}}_{\text{DD}(0)}(\underline{b})$ and $\underline{\breve{y}}_{\text{DD}(1)}(\underline{b})$ are as defined in (33) and (34), respectively.

Bit error probability calculation for the matched filter and decorrelating detectors is exponentially complex in the number of active users as it involves averaging the probability of error over the bits of all the users. A technique that allows us to rapidly analyze linear multiuser detectors in systems with larger user populations was proposed in [31]. In [31], the probability of error was calculated using moment generating functions and contour integration.

3) Performance Criterion-Based Filters: It will be observed in Section V that the Wiener and high-pass filters work well for high-rate users, but the introduction of rate-separating filters worsens the performance for the low-rate users. We provide the following intuitive explanation. In an effort to suppress the MAI due to out-of-rate users, the Wiener filter reduces the desired user's signal energy and increases correlation among users at the same rate. Furthermore, as noted earlier, ISI is introduced and the overall noise variance is increased. Assessment of the causes of poor performance gains for low-rate users shows that there are five objectives to be considered when designing filters that would achieve higher performance gains: preserving the desired user's energy, reducing the correlation between in-rate users, reducing the correlation between users of different rates, reducing the ISI, and reducing the filter output noise variance. We will see that all of the energies and correlations corresponding to these five objectives are present in the argument of the Q function in (20).

In the high signal-to-noise ratio (SNR) region, the probability of error is dominated by the Q function with the smallest argument. Therefore, considering the high SNR region, one option is to find a filter that minimizes the dominant Q function in order to reduce the probability of error for the matched filter. Similar cost functions can be derived for the decorrelator. The functions to be optimized in order to find the filter coefficients are given in [25] and [26]. We call the resulting filter the Q-filter.

For brevity, in this paper we only discuss the results and the drawbacks of designing such filters. The filter design turns out to be a nonlinear maximization problem for which a closed-form solution is not tractable. Iterative techniques are considered for seeking the desired filter. Our experience indicates that often the algorithm converges to a local maximum. While performance gains do result over the Wiener filters, the

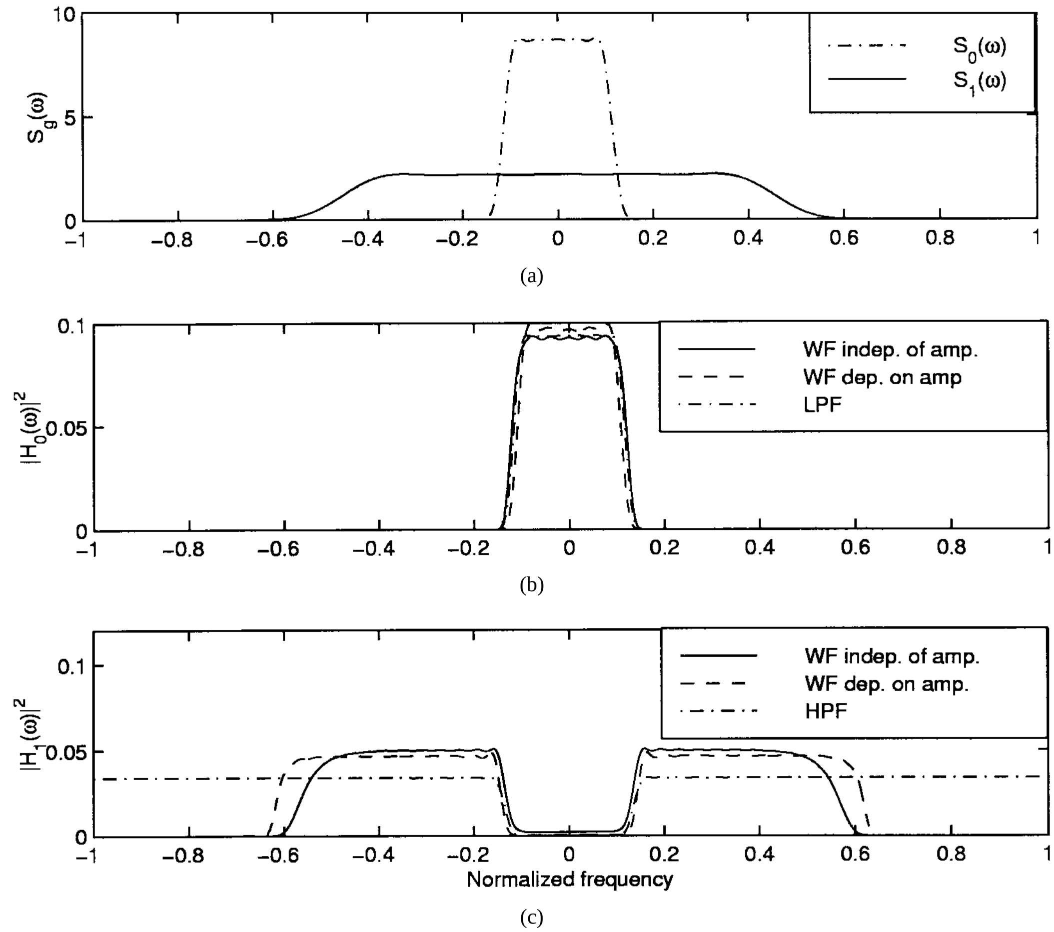

Fig. 2. (a) Normalized spectra of low-rate and high-rate users. (b) Rate-separation filter $H_0(\omega)$. (c) Rate separation filter $H_1(\omega)$.

gains are not significant and come at some computational cost. Also, it should be noted that whereas the design of the Q-filter requires the knowledge of the spreading waveform, the design of the Wiener filter does not. Thus the Q-filter can be used only at the base station and not at the mobile.

In order to overcome the problem of local maxima, cost functions that are easier to maximize are considered. One option is to have a cost function ($f_1(\underline{\mathrm{h}})$ in Fig. 10) that uses the squares of the correlations as opposed to their absolute values ($f(\underline{\mathrm{h}})$ in Fig. 10). Lower bit error rates can be achieved by weighting the five objectives in the cost function appropriately. For example, reduction of the noise variance can be emphasized by using a function $f_2(\underline{\mathrm{h}})$, which performs better than that which uses $f(\underline{\mathrm{h}})$ for low values of SNR (shown in Fig. 10).

IV. Overlay Systems

The dual-rate system considered in Section II has signals with spectrally raised cosine pulse shapes whose spectra are as shown in Fig. 2. It can be seen that the spectra of the high-rate and low-rate users are centered around the same frequency and have limited power for $|\omega| > 0.6\pi$. Also, since the bandwidth of the low-rate users is small compared to the high-rate bandwidth, the high-rate users do not have interference from the low-rate users for a large fraction of their bandwidth. This results in inefficient utilization of the frequency band allocated for the CDMA system. Hence, it may be better to overlay the low-rate users on the high-rate users such that after modulation onto the carrier, they utilize more of the high-rate frequency band [28]. Also, by modulating low-rate users onto different carriers, we can improve their performance.

There has been research on CDMA overlay situations where a CDMA system is overlaid on an existing set of very narrow-band users without adversely affecting either. Typically, these narrow-band users are not CDMA users but tone jammers or microwave users, etc. Due to the presence of narrow-band users, a double-sided Wiener filter at each CDMA receiver is employed to reject the interference in [22]. The performance of an adaptive least mean square (LMS) filter in cellular CDMA overlay situations was studied in [23]. It is shown that the performance of the adaptive LMS filter is not significantly worse than the performance of a Wiener filter, assuming that the LMS filter has had sufficient time to converge. Since past research has shown that the use of suppression filters improves the performance of the CDMA receiver in such overlay situations, we will study the performance of such filters in a situation where sets of narrow-band CDMA users (versus narrow-band interference) are overlaid on a set of wide-band CDMA users.

A. Analysis

We will analyze the performance of the rate-separation filters for this system. In the overlay system, the high-rate users' signals are the same as in Section III. But L sets of low-rate users are modulated using carrier frequencies $f_{c_1}, \ldots, f_{c_L}$. Since the signals in our system are real, we have considered double sideband amplitude modulation. The carrier frequencies are chosen such that the L sets of low-rate users are equally spaced over the high-rate bandwidth. If the high-rate users are also modulated, then $L \leq \lfloor M \rfloor$, else $L \leq \lfloor M/2 \rfloor$. The signature waveforms of the low-rate users are modified as

$$s_{k,0}^{(l)}(t) = s_{k,0}(t)\cos(2\pi f_{c_l} t); \qquad l = 1, \ldots, L \tag{37}$$

where $f_{c_i} > f_{c_j}$, $j > i$, and $s_{k,0}(t)$ is defined in (2). The superscripts refer to the lth set of low-rate users. Therefore, the spectra of the low-rate users become

$$S_0^{(l)}(f) = \frac{1}{2}\left[S_0(f - f_{c_l}) + S_0(f + f_{c_l})\right], \quad l = 1, \ldots, L \tag{38}$$

where $S_0(f)$ is defined in Section III-A2. The receiver structure proposed in Section III can be easily extended for this overlay system, as shown in Fig. 1(b). The receiver will now have $L+1$ rate-separating filters, one for the high-rate users and L for the L sets of low-rate users. For this system, the high- and low-pass filters can no longer be used as filter choices but bandpass filters can be used. The Wiener filters can also be used with appropriate modification. The Wiener equation in (5) is modified as

$$H_0^{(n)}(f) = \frac{a_0^{(n)} S_0^{(n)}(f)}{\sum_{l=1}^{L} a_0^{(l)} S_0^{(l)}(f) + a_1 M S_1(f) + S_N(f)}; \quad n = 1, \ldots, L \tag{39}$$

$$H_1(f) = \frac{a_1 M S_1(f)}{\sum_{l=1}^{L} a_0^{(l)} S_0^{(l)}(f) + a_1 M S_1(f) + S_N(f)} \tag{40}$$

where $a_0^{(l)} = \Sigma_{k=1}^{K_0^{(l)}} (a_{k,0}^{(l)})^2$ and $a_1 = \Sigma_{k=1}^{K_1} a_{k,1}^2$. The amplitudes and the number of low-rate users of set l are denoted by $a_{k,l}^{(l)}$ and $K_0^{(l)}$, respectively. The equations for the amplitude-independent Wiener filter are given by

$$H_0^{(n)}(f) = \frac{S_0^{(n)}(f)}{\sum_{l=1}^{L} \alpha_0^{(l)} S_0^{(l)}(f) + \alpha_1 S_1(f) + \alpha_N S_N(f)} \quad n = 1, \ldots, L \tag{41}$$

$$H_1(f) = \frac{S_1(f)}{\sum_{l=1}^{L} \alpha_0^{(l)} S_0^{(l)}(f) + \alpha_1 S_1(f) + \alpha_N S_N(f)}. \tag{42}$$

We have chosen $\alpha_0^{(l)} = \alpha_1 = \alpha_N = 1$; $l = 1, \ldots, L$. Since this system fits in the framework of Section III, no additional analysis is needed and the results of Section III-B can be used.

B. Design of High-Rate Chip Pulse

It will be observed in Section V that the performance of the set of low-rate users having a higher carrier frequency was close to the single-user bound, while that of the low-rate users modulated on to a lower carrier frequency was poor. The difference in performance is due to the PSD of the high-rate users' being concentrated at low frequencies. As a result of this, one set of low-rate users suffer from strong out-of-rate interference while the other has less out-of-rate interference. Therefore, we next explore the design of high-rate chip pulse shape such that both sets of low-rate users experience low out-of-rate interference. Honig and Roy have considered the problem of optimizing the transmitter pulse shaping filters for each user assuming different symbol rates [7]. They assumed the minimum mean squared error performance criteria and derived necessary conditions for optimality. However, they placed no constraints on the resulting ISI. There have been other papers on design of pulse shape for MSK-type signals [29] and partial response signalling systems [30]. The design criteria vary according to the system under consideration. However, in general, the bandwidth occupied by the pulse, the pulse duration and the ISI introduced by the pulse are major concerns. For our system, one option is to find a pulse shape that minimizes the correlation between the PSD's of the high-rate users and the PSD's of the L sets of low-rate users. In addition to this, we would like the high-rate chip pulse to be essentially band-limited. In other words, the high-rate chip pulse $\tilde{p}_1(t)$ is designed such that the following expression is minimized:

$$\int_{-\infty}^{\infty} S_0^{(1)}(f)\tilde{S}_1(f)\,df + \int_{-\infty}^{\infty} S_0^{(2)}(f)\tilde{S}_1(f)\,df + \cdots + \int_{-\infty}^{\infty} S_0^{(L)}(f)\tilde{S}_1(f)\,df + \lambda \int_{(1+\alpha)/T_{c_1}}^{\infty} |\tilde{X}_1(f)|^2\,df \tag{43}$$

where $S_0^{(l)}(f)$ is defined in Section III-A2, $l = 1, \ldots, L$. The power spectrum and the Fourier transform of the pulse $\tilde{p}_1(t)$ are denoted by $\tilde{S}_1(f)$ and $\tilde{X}_1(f)$, respectively. The performance of the proposed receiver structure will be investigated for this pulse. The Wiener equations are same as in (39)–(42), however with $S_1(f)$ replaced by $\tilde{S}_1(f)$. The performance analysis is similar to Section III-B assuming that the intersymbol interference is less than a high-rate bit interval. A high-rate chip pulse of length $\tilde{T}_1 = 1.25T_{c_1}$ is designed using $\lambda = 1$. The spectra are shown in Fig. 14. It is clear that the design specification dramatically reduces the correlation between users of different rates. Furthermore, the resulting spectrum is reminiscent of multicarrier DS-CDMA transmission [32], [33]. The narrow-band interference suppression abilities of multicarrier systems have been explored in [32] and [33]. The resulting spectra indicate that the use of a multicarrier DS-CDMA system as an implementation for a multirate CDMA system merits further investigation and may be the implementation of choice to achieve moderate complexity.

V. Numerical Results

In this section, the performance of the single-rate receivers with filtering will be compared to that without any filtering. The performance will also be compared to the single-user bound, which gives the optimal performance. Let us consider an asynchronous CDMA system, which supports fourteen users where $K_0 = 7$ and $K_1 = 7$ with rate ratio $M = 4$. The processing gain for all the users is $N = 63$. The performance of the low- and high-rate users is studied for particular sets of delays of the users, which are chosen randomly. Gold codes are used as signature sequences.

For our analysis, the signal is sampled at a frequency four times that of the fundamental frequency of the high-rate users, i.e., $f_s = 4/T_{c_1}$. Since the rate ratio is four, the sampling frequency is 16 times that of the fundamental frequency of the low-rate signal $f_s = 16/T_{c_0}$. The sampled signals have periodic spectra $S_g(\omega)$, shown in Fig. 2. The normalized frequency of 1 in Fig. 2 corresponds to $f_s/2$. Since the analog signal is essentially band-limited and sampled above the Nyquist rate, the aliasing errors due to sampling are negligible. Four scenarios are considered: single-carrier systems, Q-filter designs, overlay systems, and overlay systems with high-rate pulse shaping.

A. Single-Carrier Systems

High- and low-pass finite impulse response (FIR) digital filters are designed using the Kaiser window with $\beta = 5$. The Wiener filters and the amplitude-independent Wiener filters are found using (5) and (7), respectively. The Wiener filters are implemented as linear-phase, FIR filters that are the best least squares approximation to the desired frequency response $H_g(f)$ for a given filter length. The discrete-time frequency responses of the filters used for rate separation are shown in Fig. 2.

Fig. 3 shows the bit error probability (BEP) for the first high-rate user as a function of SNR.[2] The amplitudes of the high-rate users are fixed at one and those of the low-rate users are fixed at four. The performance of the receiver with the Wiener filter and with a high-pass filter is shown. The filter lengths have been chosen to be $25.25T_{c_1}$, as the performance did not improve for larger values of filter length. With the high-pass filter, the performance of the receiver for various cutoff frequencies was observed, and it was found that a cutoff of 0.1275π yielded the best result. The chosen cutoff is also in accordance with the cutoff frequency given in Section III-A1. This cutoff frequency is specific for a rate ratio of four. It is clear that the suppression of interference due to the low-rate users' using filters improves the performance for the high-rate user.

It was found that the filters reduce the energy of the desired user, increase the in-rate correlation and the variance of the noise, in an effort to suppress the MAI due to other rate users. Therefore, the overall gain due to filtering is the gain in reducing the out-of-rate interference over the loss in increasing the other interference terms, such as ISI, additive noise, and in-rate interference. It can be observed that the overall gain for the Wiener filter is less than that of the amplitude-independent Wiener filter for SNR's ranging from 0 to 14 dB. A whitening filter was also analyzed and it was found to have a performance worse than the Wiener filter.

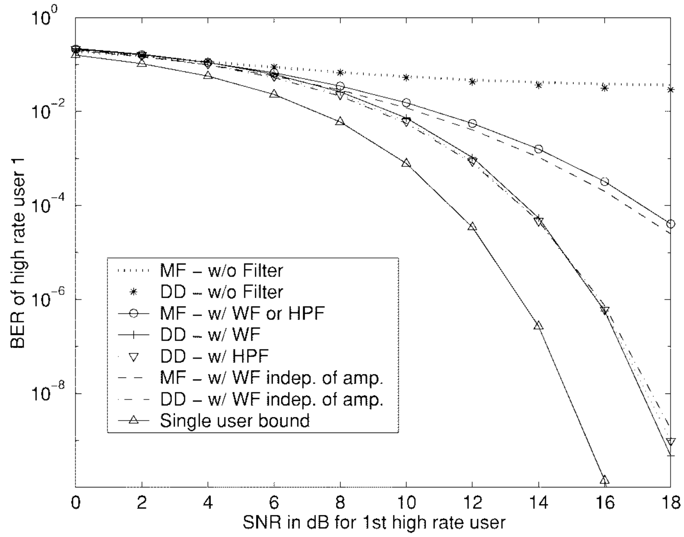

Fig. 3. High-rate user performance as a function of SNR. $K_0 = 7, K_1 = 7$; $a_{k,1} = 1$, $a_{k,0} = 4$; $M = 4$.

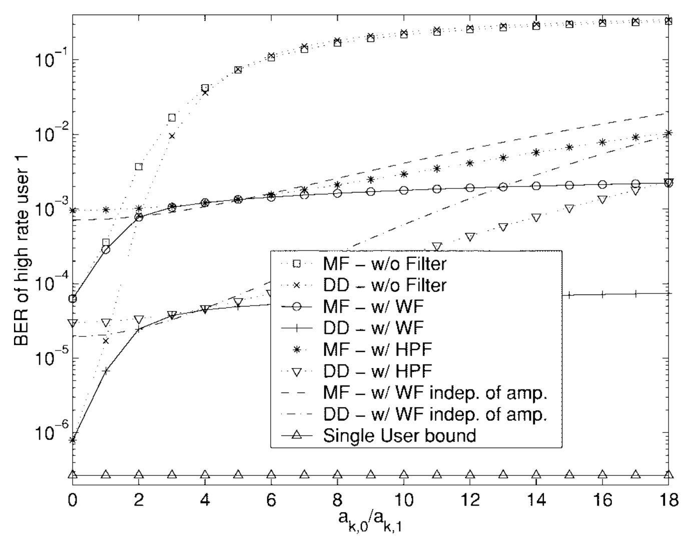

Fig. 4. High-rate user performance as a function of near–far ratio. $K_0 = 7$, $K_1 = 7$; SNR = 14 dB; $M = 4$.

Fig. 4 shows the BEP of the high-rate user as a function of the amplitude ratio with the SNR fixed at 14 dB. When the interference due to the low-rate users is low $(a_{k,0}/a_{k,1} < 2)$, the receiver without any filter performs better than those with amplitude-independent filters. This is due to the fact that the overall gain due to filtering is less than unity in this region. Here, we can see that the amplitude-dependent Wiener filter performs better than the amplitude-independent filters except over a range $2 < a_{k,0}/a_{k,1} < 5$, as it is able to adapt to changes in the near–far ratio. Also, since the decorrelator zero-forces only the same rate interferers, the decorrelator is near–far limited.

The performance of the high-rate user is studied as a function of the rate ratio M with $K_0 = 2$ and $K_1 = 2$. The

[2] The SNR in dB is calculated as $10 \log_{10}(1/\sigma^2)$ since the amplitude of the desired user is fixed at 1.

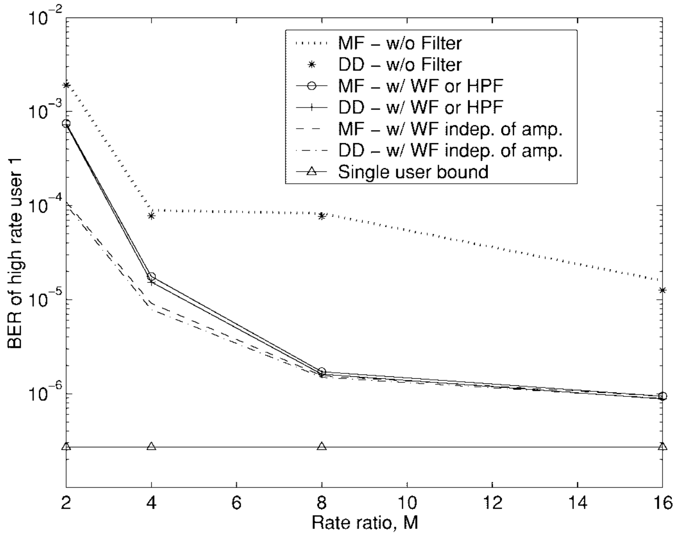

Fig. 5. High-rate user performance as a function of rate ratio. $K_0 = 2$, $K_1 = 2$; $a_{k,1} = 1$, $a_{k,0} = 4$; SNR = 14 dB.

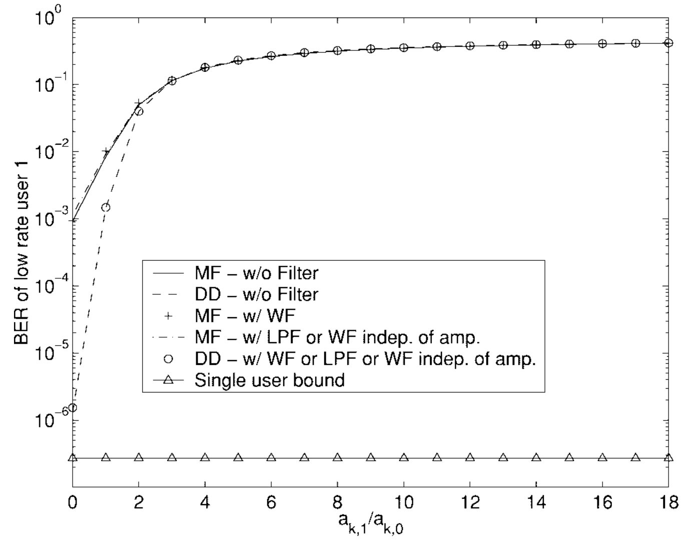

Fig. 6. Low-rate user performance as a function of near–far ratio. $K_0 = 7$, $K_1 = 7$; SNR = 14 dB; $M = 4$.

amplitudes are chosen to be one for the high-rate users and four for the low-rate users. The SNR is 14 dB. As the rate ratio is increased, the range of frequencies for which the high-rate and low-rate spectra overlap decreases. This causes the BEP of both receivers with and without filter to decrease and is shown in Fig. 5. Looking at the time domain, as the rate ratio increases, the energy of a low-rate user in a high-rate interval decreases due to the normalization of the signature waveforms. This gives an alternate interpretation for the decrease in the BEP with increase in rate ratio. It can be observed that the BEP curve of the receiver without filtering is not smooth. This is due to the variation in the cross-correlation values of the high-rate user for different subintervals of a low-rate user, as the rate ratio is varied. Since the rate-separation filter significantly reduces the low-rate interference, the BEP curve for receivers that use Wiener or high-pass filters is smooth. As expected, the BEP of the high-rate user increased as the number of users in each rate was increased.

For the high-rate users, the inclusion of a rate-separation filter at the front end of a matched filter or a decorrelator improves the performance significantly. Therefore, the proposed receiver can be used at both the base station and the mobile to improve the performance of detecting high-rate users, however with a slight increase in complexity.

The performance of the low-rate users is presented in Figs. 6 and 7. The low-rate filter lengths have been chosen to be $25.25T_{c_1}$, and the cutoff frequency for the low-pass filter was chosen as 0.125π. It was observed that the performance of the receiver with this filter is almost the same as that without any filter, and sometimes even worse. This is due to the high interference caused by the high-rate users over the entire band of the low-rate spectrum. Therefore, the filter is unable to suppress the interference due to other-rate users while introducing ISI and increasing the variance of the noise. Moreover, since the high-rate spectrum is almost flat over the low-rate band, it is close to white noise, in which case the single-rate decorrelator would perform the best. It can be observed that the BEP of the low-rate users as a function of rate ratio has pathological behavior. This behavior can be attributed to the change in the cross-correlation values. Moreover, the energy of a high-rate user in a low-rate interval increases linearly with M. This causes an overall increase in BEP as the rate ratio increases.

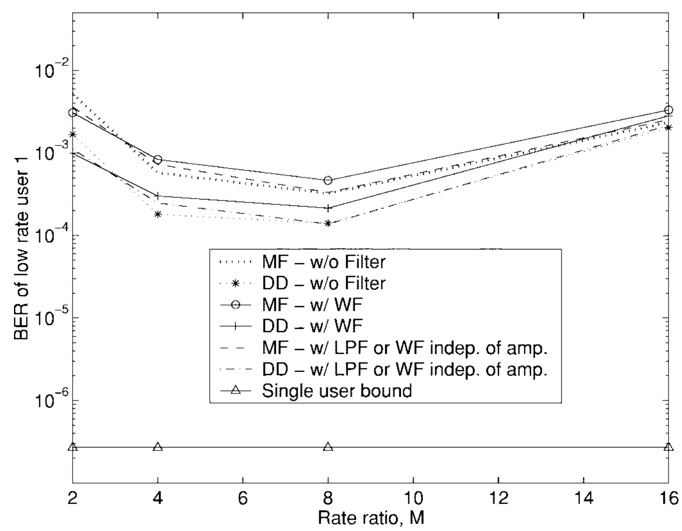

Fig. 7. Low-rate user performance as a function of rate ratio. $K_0 = 2$, $K_1 = 2$; $a_{k,0} = 1$, $a_{k,1} = 2$; SNR = 14 dB.

In order to show that the proposed receiver can be extended to a multirate system, we will consider a system with three different rates. The number of users in each rate is chosen to be four, and the rate ratios are fixed as $M_1 = 4$ and $M_2 = 16$ $(M_0 = 1)$. The spectra of users of different rates is shown in Fig. 8. The performance of the highest and the lowest rate users are found to be similar to that of the high- and low-rate users of the dual-rate system. The performance of users of medium rate is shown in Fig. 9. The performance of the medium-rate user lies in between that of the highest and the lowest rate users. Also, it can be observed that the rate-separation filters improve performance in the case of the medium-rate user. Thus we can conclude that rate-separation

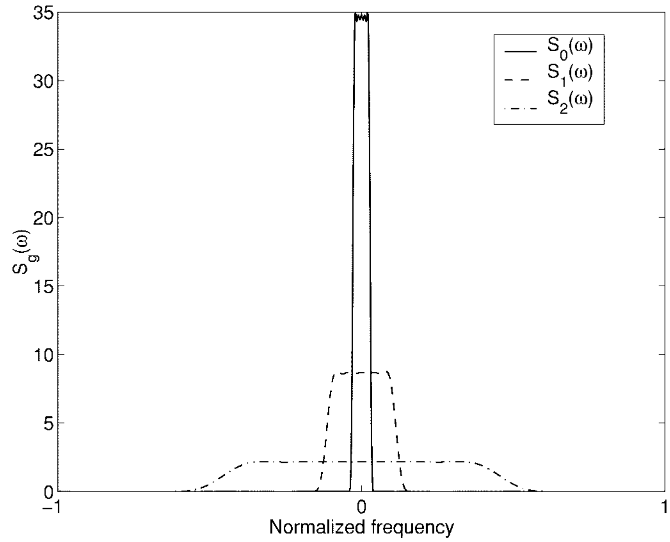

Fig. 8. Spectra of users for $G = 3$, $M_1 = 4$, and $M_2 = 16$.

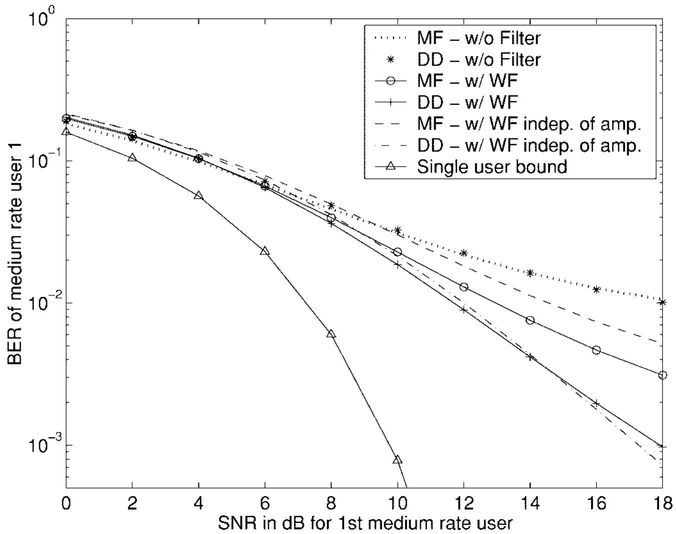

Fig. 9. Medium rate users' performance as a function of SNR. $K_0 = 4$, $K_1 = 4$, $K_2 = 4$; $a_{k,1} = 1$, $a_{k,0} = a_{k,2} = 2$; $M_1 = 4$, $M_2 = 16$.

will improve performance of the higher rate users, while the lower rate users could suffer.

B. Q-Filters

The performance of the receiver with a Q-filter design as discussed in Section III-B3 is presented for a synchronous dual-rate CDMA system with $K_0 = 2$ and $K_1 = 2$ with rate ratio $M = 4$. It is observed that the performance of the receiver with the Q-filter is slightly better than that with the Wiener filter for high values of SNR. The performance of the Q-filter for the low-rate users is shown in Fig. 10. As the Q-filter with $f(h)$ is designed to reduce the BEP for high values of SNR, we can see that its performance is better than other rate-separation filters for SNR > 13 dB. Though the function $f_1(h)$ is easier to maximize, its performance is worse when compared to using $f(h)$ or $f_2(h)$ but is still better than the Wiener filter. Finally, the weighting of the noise variance in $f_2(h)$ helps to reduce the BEP for low values of SNR, but the BEP is higher than with $f(h)$ for SNR > 16 dB. The Q-filters thus can provide some improvement for low-rate users, but this improvement is not always significant.

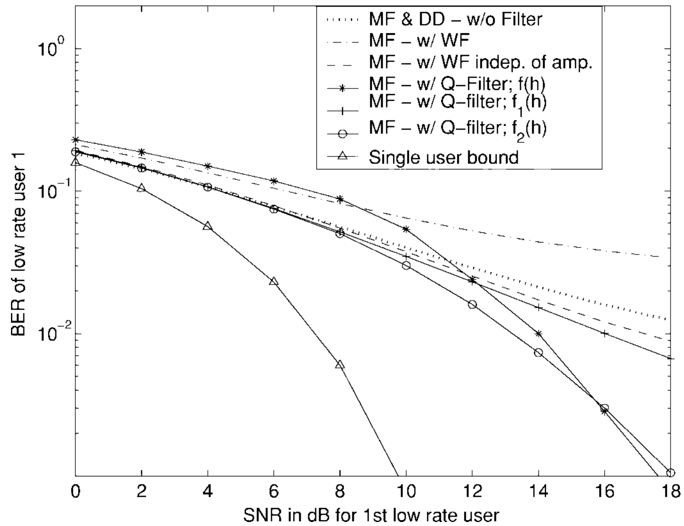

Fig. 10. Low-rate user performance as a function of SNR. $K_0 = 2, K_1 = 2$; $a_{k,0} = 1$, $a_{k,1} = 4$; $M = 4$.

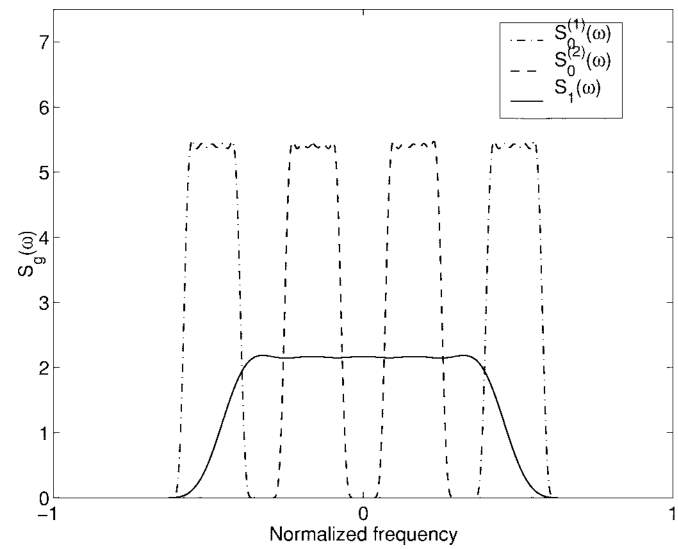

Fig. 11. Spectra of low-rate and high-rate users in a CDMA overlay situation for $M = 5$ and $L = 2$.

C. Overlay Systems

We next consider the performance of the receiver for an asynchronous system with seven users per rate as before, but now the seven low-rate users are separated into two sets. Four low-rate users are modulated onto a higher carrier frequency (i.e., $K_0^{(1)} = 4$) such that they have a spectrum $S_0^{(1)}(\omega)$ as shown in Fig. 11. The other three low-rate users are modulated onto a lower carrier frequency $(K_0^{(2)} = 3)$ and have a spectrum $S_0^{(2)}(\omega)$. The rate ratio considered for this analysis is five. Fig. 12 shows the performance of a high-rate user as a function of SNR. The performance of the receiver that uses a rate-separation filter shows that it is better than using just a single-rate detector. However, since the high-rate

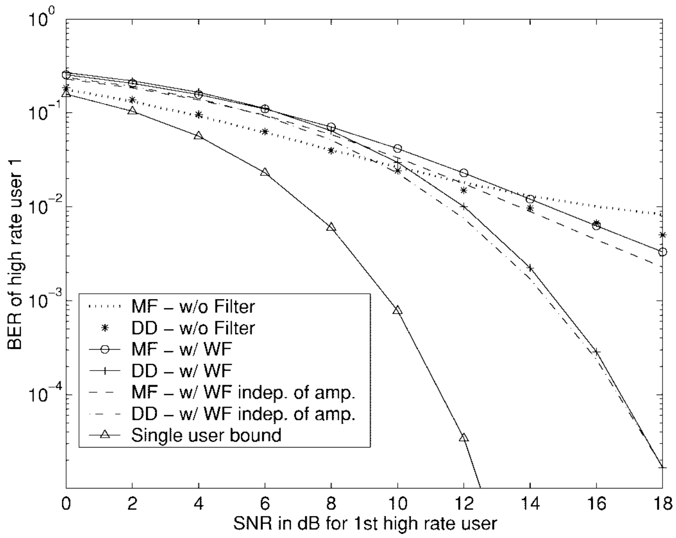

Fig. 12. High-rate user performance as a function of SNR. $K_0^{(1)} = 4$, $K_0^{(2)} = 3$, $K_1 = 7$; $a_{k,1} = 1$, $a_{k,0}^{(1)} = a_{k,0}^{(2)} = 4$; $M = 5$.

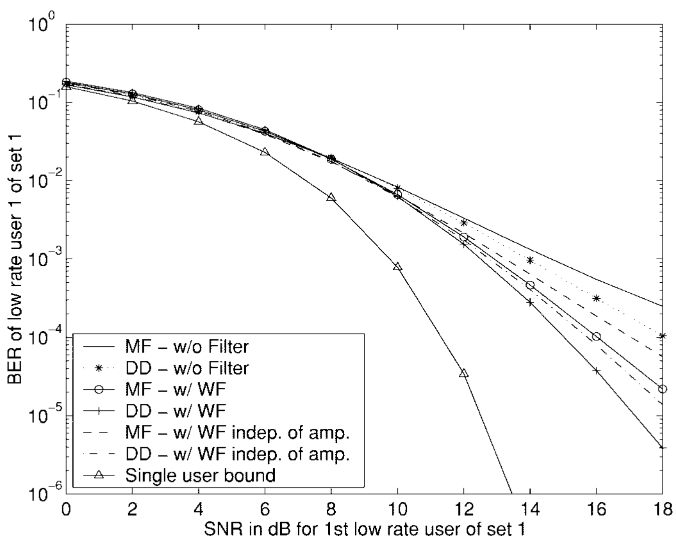

Fig. 13. Performance of a low-rate user with higher carrier frequency as a function of SNR. $K_0^{(1)} = 4$, $K_0^{(2)} = 3$, $K_1 = 7$; $a_{k,0}^{(1)} = 1$, $a_{k,0}^{(2)} = 2$, $a_{k,1} = 2$; $M = 5$.

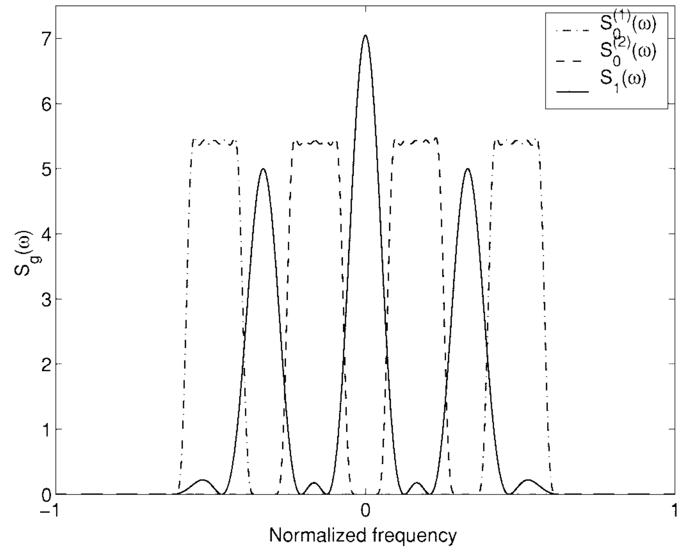

Fig. 14. Spectra of low-rate and high-rate users in a CDMA overlay situation for $M = 5$ and $L = 2$.

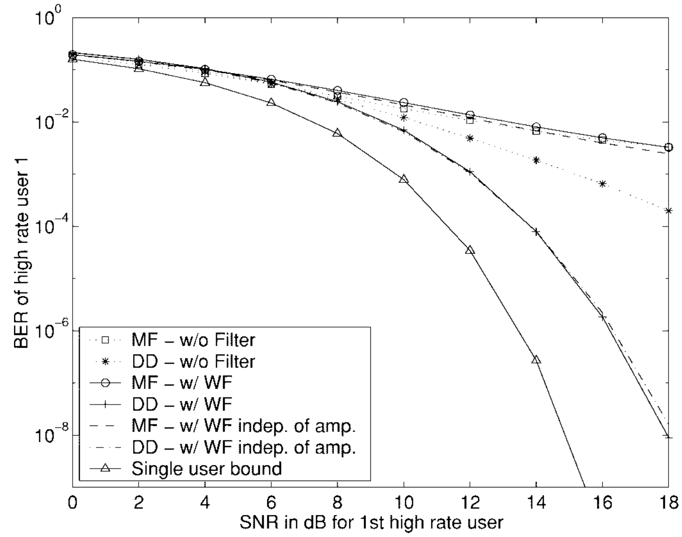

Fig. 15. High-rate user performance as a function of SNR. $K_0^{(1)} = 4$, $K_0^{(2)} = 3$, $K_1 = 7$; $a_{k,1} = 1$, $a_{k,0}^{(1)} = a_{k,0}^{(2)} = 4$; $M = 5$.

users now experience interference from the low-rate users over their entire bandwidth, the performance of the high-rate users is worse when compared to that in the original system shown in Fig. 3. The performance of a low-rate user with higher carrier frequency is shown in Fig. 13. It can be seen that the BEP of the low-rate user is closer to the single-user bound when compared to the original system, as there is less high-rate interference. The receiver with a Wiener filter performs better than that without any rate-separation filter. The performance of a low-rate user with lower carrier frequency is poor due to the strong out-of-rate interference. It is clear that by reducing interference, an overlay system can aid in improving the BEP for low-rate users.

D. Overlay Systems with High-Rate Pulse Shaping

A high-rate chip pulse of length $\tilde{T}_1 = 1.25T_{c_1}$ is designed using $\lambda = 1$. Fig. 15 shows the performance of the high-rate users as a function of SNR. The amplitude of the high-rate users is fixed at one and that of the low-rate users at four. It can be noted that the receiver with a rate-separation filter followed by a decorrelating detector performs better than a receiver with only a decorrelator. The high-rate chip pulse is designed such that the correlation with out-of-rate users is minimized. However, this increases the in-rate correlation. It can be seen that the rate-separation filter followed by a matched filter performs the worst. The performance of the first low-rate user of set 1 (shown in Fig. 16) is close to the single-user bound, as there is negligible interference from the high-rate users. Since there is negligible out-of-rate interference, there is only slight improvement in performance by using rate-separation filters. The amplitude-dependent Wiener filter worsens the performance by reducing the desired user's energy. Finally, the BEP for the first low-rate user of set 2 is shown as a

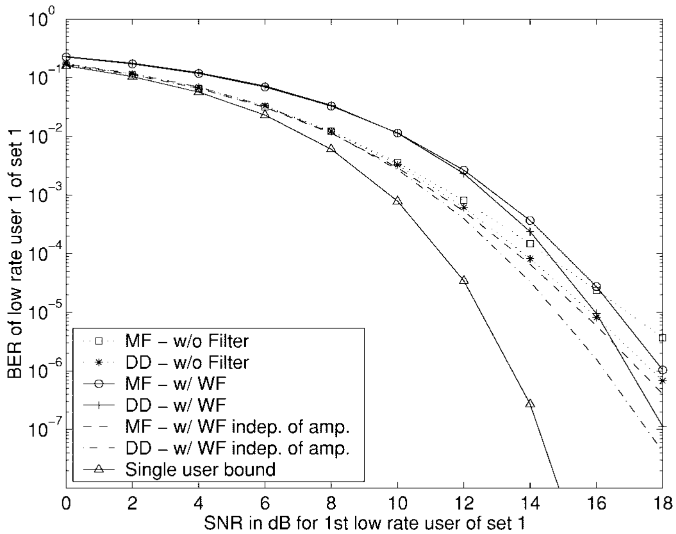

Fig. 16. Performance of a low-rate user with higher carrier frequency as a function of SNR. $K_0^{(1)} = 4$, $K_0^{(2)} = 3$, $K_1 = 7$; $a_{k,0}^{(1)} = 1$, $a_{k,0}^{(2)} = 2$, $a_{k,1} = 2$; $M = 5$.

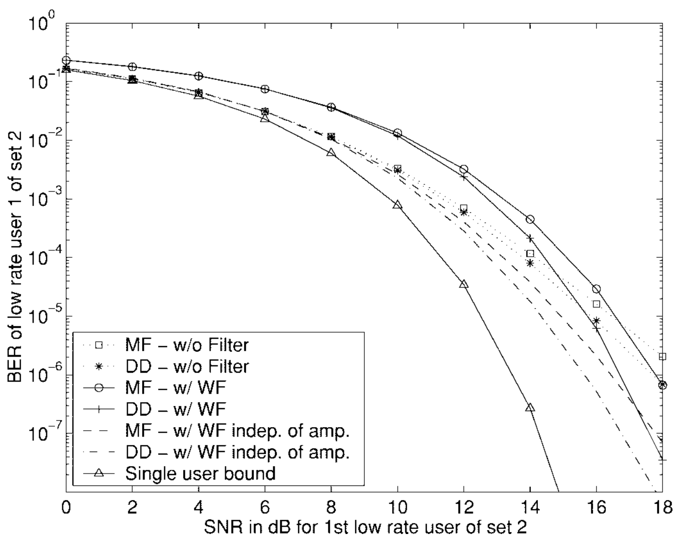

Fig. 17. Performance of a low-rate user with lower carrier frequency as a function of SNR. $K_0^{(1)} = 4$, $K_0^{(2)} = 3$, $K_1 = 7$; $a_{k,0}^{(2)} = 1$, $a_{k,0}^{(1)} = 2$, $a_{k,1} = 2$; $M = 5$.

function of SNR in Fig. 17. For this set of users we can observe significant improvement in performance by using the new pulse for the high-rate users. Also, it can be observed that all the low-rate users have similar performance. Though the rate-separation filter followed by a matched filter does not offer much improvement in performance compared to the single-rate decorrelator, it is of much lower complexity. Thus it is best suited to be used at the mobile.

VI. Conclusion

In this paper, we have considered low-complexity receivers for multirate, multiuser systems. The proposed receivers use filters to achieve user separation by rate, followed by single-rate multiuser detection. We have shown that the proposed receivers for a common carrier multirate system offer improved performance in the detection of high-data-rate users when compared to single-rate detectors, which are matched only to the rate of interest. Such single-rate matched filters or decorrelators ignore the out-of-rate users. However, performance improvement for low-rate users was modest at best when compared to the single-rate detectors, as separation by rate does not afford any significant suppression of interference power.

Performance gain was observed for the low-rate users when criterion-based filters (Q-filters) were employed. However such filters were of higher complexity to calculate, requiring nonlinear maximization, and required complete spreading code information; this limits their practical use at the mobile. Furthermore, optimization of the designs was difficult due to convergence to local maxima.

To improve bandwidth efficiency and to potentially improve performance of the low-rate users, an overlay scenario was investigated. The performance gains afforded the low-rate users were not uniform due to the fact that the high-rate interference power was not uniformly distributed across the bandwidth of interest. A further system modification was implemented, using pulse shaping of the high-rate users' chip pulses to equalize the performance of the low-rate users.

The feasibility and strong performance of a moderate-complexity, multirate system employing frequency-based rate separation, overlay ideas, and pulse shaping has been shown. Both high- and low-rate users can achieve good probabilities of error. The rate-separating filters of interest were of Wiener type and were independent of the exact realizations of spreading codes; thus these filters can be employed at either the base station or the mobile. Finally, it should be noted that as the bandwidth of the users will remain the same in a multipath channel, the proposed rate-separation technique can be applied to multipath channels in conjunction with the appropriate multipath multiuser detector.

Acknowledgment

The authors wish to thank Prof. R. Pickholtz of George Washington University for suggesting the investigation of improved pulse shapes for the high-rate users.

References

[1] R. Lupas and S. Verdú, "Linear multiuser detectors for synchronous Code-Division Multiple-Access channels," *IEEE Trans. Inform. Theory*, vol. 35, pp. 123–136, Jan. 1989.

[2] M. K. Varanasi and B. Aazhang, "Near-optimum detection in synchronous code-division multiple-access systems," *IEEE Trans. Commun.*, vol. 39, pp. 725–736, May 1991.

[3] A. Duel-Hallen, "Decorrelating decision-feedback multiuser detector for synchronous code-division multiple-access channels," *IEEE Trans. Commun.*, vol. 41, pp. 285–290, Feb. 1993.

[4] U. Madhow and M. L. Honig, "MMSE interference suppression for direct-sequence spread spectrum CDMA," *IEEE Trans. Commun.*, vol. 42, pp. 3178–3188, Dec. 1994.

[5] S. Verdú, "Minimum probability of error for asynchronous Gaussian multiple-access channels," *IEEE Trans. Inform. Theory*, vol. IT-32, pp. 85–96, Jan. 1986.

[6] M. J. McTiffin, A. P. Hulbert, T. J. Ketseoglou, W. Heimsch, and G. Crisp, "Mobile access to an ATM network using CDMA air interface," *IEEE J. Select. Areas Commun.*, vol. 12, pp. 900–908, June 1994.

[7] M. L. Honig and S. Roy, "Multi-user communication with multiple symbol rates," in *Proc. IEEE Int. Symp. Information Theory*, Whistler, B.C., Canada, Sept. 1995, p. 381.
[8] C.-L. I, G. P. Pollini, L. Ozarow, and R. D. Gitlin, "Performance of multi-code CDMA wireless personal communications networks," in *Proc. IEEE Vehicular Technology Conf.*, Chicago, IL, July 1995, pp. 907–911.
[9] T. Ottosson and A. Svensson, "On schemes for multirate support in DS-CDMA systems," *J. Wireless Personal Commun.*, vol. 6, no. 3, pp. 265–287, Mar. 1998.
[10] E. Geraniotis, Y.-W. Chang, and W.-B. Yang, "Dynamic code allocation for integrated voice and multi-priority data traffic in CDMA networks," *Eur. Trans. Telecommun.*, vol. 6, no. 1, pp. 85–96, Jan.–Feb. 1995.
[11] F. Adachi, M. Sawahashi, and H. Suda, "Wideband DS-CDMA for next-generation mobile communication systems," *IEEE Commun. Mag.*, pp. 56–69, Sept. 1998.
[12] E. Dahlman, B. Gudmundson, M. Nilsson, and J. Sköld, "UMTS/IMT2000 based on wideband CDMA," *IEEE Commun. Mag.*, pp. 70–80, Sept. 1998.
[13] R. Wyrwas, M. J. Miller, R. Anjaria, and W. Zhang, "Multiple access options for multi-media wireless systems," in *Proc. 3rd Workshop Third Generation Wireless Information Networks*, WINLAB, Rutgers Univ., New Brunswick, NJ, Apr. 1992, pp. 289–294.
[14] T.-H. Wu and E. Geraniotis, "CDMA with multiple chip rates for multi-media communications," in *Proc. 28th Annu. Conf. Information Sciences and Systems*, Princeton, NJ, Mar. 1994, pp. 992–997.
[15] M. Saquib, R. Yates, and N. Mandayam, "Decorrelating detectors for a dual rate synchronous DS-CDMA channel," *Wireless Personal Commun.*, to be published.
[16] U. Mitra and J. Chen, "Further results for multi-rate decorrelators for synchronous DS-CDMA systems," in *Proc. 34th Annu. Allerton Conf.*, Monticello, IL, Oct. 1996, pp. 170–179.
[17] U. Mitra, "Comparison of ML-based detection for two multi-rate access schemes for CDMA signals," *IEEE Trans. Commun.*, vol. 47, pp. 64–77, Jan. 1999.
[18] A.-L. Johansson and A. Svensson, "Successive interference cancellation schemes in multi-rate DS-CDMA systems," *Kluwer International Series in Engineering and Computer Science*, no. 351, p. 265, 1996.
[19] J. G. Proakis and M. Salehi, *Communication Systems Engineering*. Englewood Cliffs, NJ: Prentice-Hall, 1994, pp. 553–554.
[20] R. A. Iltis and L. B. Milstein, "Performance analysis of narrow-band interference rejection techniques in DS spread-spectrum systems," *IEEE Trans. Commun.*, vol. COM-32, pp. 1169–1177, Nov. 1984.
[21] E. Masry and L. B. Milstein, "Performance of DS spread-spectrum receiver employing interference-suppression filters under a worst case jamming condition," *IEEE Trans. Commun.*, vol. COM-34, pp. 13–21, Jan. 1986.
[22] J. Wang and L. B. Milstein, "CDMA overlay situations for microcellular mobile communications," *IEEE Trans. Commun.*, vol. 43, pp. 603–614, Feb./Mar./Apr. 1995.
[23] ——, "Adaptive LMS filters for cellular CDMA overlay situations," *IEEE J. Select. Areas Commun.*, vol. 14, pp. 1548–1559, Oct. 1996.
[24] D. Cruickshank, "Suppression of multiple access interference in a DS-CDMA system using Wiener filtering and parallel cancellation," *Proc. Inst. Elect. Eng.*, vol. 143, no. 4, pp. 226–230, Aug. 1996.
[25] R. Srinivasan, U. Mitra, and R. L. Moses, "Frequency-based rate separation for dual-rate CDMA signals," in *Proc. Conf. Information Sciences and Systems*, Princeton, NJ, Mar. 1998, vol. 1, pp. 163–168.
[26] R. Srinivasan, "Frequency-based detection schemes for multi-rate direct sequence code division multiple access systems," M.S. thesis, The Ohio State Univ., Columbus, OH, 1998.
[27] S. Verdù, *Multi-User Detection*. New York: Cambridge Univ. Press, 1998.
[28] I. Oppermann and M. Latva-aho, "Multiple traffic type CDMA systems using an improved adaptive LMMSE receiver," in *Proc. IEEE Int. Symp. Information Theory*, Ulm, Germany, 1997, p. 358.
[29] A. J. Vigil, M. A. Belkerdid, and D. C. Malocha, "Results of optimal discrete pulse shaping for MSK-type signals," *IEEE Trans. Commun.*, vol. 44, pp. 769–771, July 1996.
[30] A. Grami and S. Pasupathy, "Pulse shape, excess bandwidth and timing error sensitivity in PRS systems," *IEEE Trans. Commun.*, vol. COM-35, pp. 475–480, Apr. 1987.
[31] S. V. Uppala, "Analysis and synthesis of linear multiuser detectors," Ph.D. dissertation, Univ. Washington, Seattle, 1998, ch. 3.
[32] D. N. Rowitch and L. B. Milstein, "Coded multicarrier code division multiple access," in *Proc. IEEE Int. Symp. Information Theory*, Whistler, B.C., Canada, 1995, p. 23.
[33] S. Kondo and L. B. Milstein, "Performance of multicarrier DS CDMA systems," *IEEE Trans. Commun.*, vol. 44, pp. 238–246, Feb. 1996.

Radha Srinivasan received the B.E. degree in electronics and communication from Anna University, India, in 1996 and the M.S. degree in electrical engineering from The Ohio State University, Columbus, in 1998.

Since then, she has been with Nokia Research Center, Dallas, TX as a Research Engineer. Currently, she is working on third generation mobile radio communication systems.

Ms. Srinivasan was the recipient of Ohio State University's Gold Medal Award for academic achievement. She was also the recipient of a 1996 Ohio State University Graduate Fellowship.

Urbashi Mitra (M'87) received the B.S. and M.S. degrees from the University of California, Berkeley in 1987 and 1989, respectively, both in electrical engineering and computer science, and the Ph.D. degree in electrical engineering from Princeton University, Princeton, NJ, in 1994.

From 1989 until 1990, she was a Member of Technical Staff at Bellcore, Red Bank, NJ. She is currently an Assistant Professor in the Department of Electrical Engineering at The Ohio State University, Columbus. Her current research interests include code division multiple access communications for personal wireless and mobile applications, multirate and robust systems, adaptive algorithms, and blind equalization techniques. During Summer 1995, November 1996, June 1997, and September 1997, she was a Visiting Scholar at the Institut Eurecom, Sophia Antipolis, France.

Prof. Mitra received a 1996 National Science Foundation CAREER award. She also received the 1997 Charles E. MacQuigg Award for Outstanding Teaching. She is an Associate Editor for the IEEE TRANSACTIONS ON COMMUNICATIONS and the Membership Chair for the IEEE Information Theory Society.

Randolph L. Moses (S'78–M'85–SM'90) received the B.S., M.S., and Ph.D. degrees in electrical engineering from Virginia Polytechnic Institute and State University, Blacksburg, in 1979, 1980, and 1984, respectively.

During the summer of 1983, he was an SCEEE Summer Faculty Research Fellow at Rome Air Development Center, Rome, NY. From 1984 to 1985, he was with the Eindhoven University of Technology, Eindhoven, The Netherlands, as a NATO Postdoctoral Fellow. Since 1985, he has been with the Department of Electrical Engineering, Ohio State University, Columbus, and he is currently a Professor there. During 1994–1995, he was on sabbatical leave as a Visiting Researcher at the System and Control Group at Uppsala University, Sweden. His research interests are in digital signal processing and include parametric time series analysis, radar signal processing, sensor array processing, and communications systems.

Dr. Moses served on the Technical Committee on Statistical Signal and Array Processing of the IEEE Signal Processing Society from 1991–1994. He is a member of Eta Kappa Nu, Tau Beta Pi, Phi Kappa Phi, and Sigma Xi.